Atomic multiwave interferometer in an optical lattice

Min-Kang Zhou, Bruno Pelle, Adèle Hilico, and Franck Pereira dos Santos*
LNE-SYRTE, Observatoire de Paris, LNE, CNRS, UPMC, 61 avenue de l'Observatoire, 75014 Paris, France
(Received 8 May 2013; published 3 July 2013)

A multiwave atom interferometer using multiple Wannier-Stark states is experimentally realized in a vertical optical lattice. Atoms are coherently driven by stimulated Raman transitions into a superposition of several adjacent lattice sites, in which they evolve at multiples of Bloch frequency in the same internal state to form an interference pattern. We observe coherent evolution for more than 500 Bloch periods. The noise analysis shows that the phase resolution of this interferometer is detection noise limited. This multiwave interferometer could be a potential instrument for gravimetry and short-range forces measurement.

DOI: 10.1103/PhysRevA.88.013604 PACS number(s): 37.25.+k, 32.80.Qk, 37.10.Jk, 05.60.Gg

I. INTRODUCTION

In the past decade, matter wave interferometers with impressive sensitivities have been developed, opening up new perspectives in high precision measurements and tests of fundamental physics [1,2]. Atom interferometers (AI) with cold atoms and well-controlled laser pulses, such as Mach-Zehnder [3] and Ramsey-Bordé [4] AI, have been realized and demonstrated to be powerful tools for inertial sensors and precision measurements [5–10]. These two types of interferometers are typical examples of two-wave AI. Other types of AI based on multiple waves have also been proposed [11] and demonstrated [12–17]. Multiwave atom interferometers exhibit sharper fringe patterns [12], which enables one to improve the resolution compared to those of the corresponding two-wave interferometers.

For example, multiwave interferometers with trapped atoms in optical lattices have been studied [18–20], employing Bloch oscillations. Manipulation of cold atoms trapped in optical lattices indeed provides an attractive system for metrology [21–24], simulation of solid state physics [25–28], and quantum information processes [29]. Precisely monitoring Bloch oscillations of cold atoms trapped in optical lattice has proven to be a useful tool for gravity measurements [30,31] and fine structure constant determination [23,32,33]. Also, several schemes based on lattice trapped atoms were proposed to measure short-range forces such as the Casimir-Polder force and to realize tests of Newtonian inverse-square law between an atom and a massive surface [34–38], and it would be interesting to use such a multiwave interferometer as a sensitive sensor in these experiments.

In this paper, we describe an experimental demonstration of a time domain atomic multiwave interferometer. In our experiment, ^{87}Rb atoms trapped in a shallow vertical optical lattice are manipulated using Raman transitions [39,40]. A couple of such Raman laser pulses coherently drive transitions between Wannier-Stark (WS) states, allowing tunneling of atoms between neighboring sites of the optical lattice [Fig. 1(a)]. Between these two pulses, atoms are in a superposition of WS states. Each WS state is a partial matter wave, which evolves with a phase of $\phi_m = 2\pi m \nu_B t$ (m is well index representing different wave components, $\nu_B = m_a g \lambda_l / 2h$ is the Bloch frequency, where m_a is the atom mass, g is the gravitational acceleration, and λ_l is the lattice wavelength). These waves rephase at every Bloch period $T_B = 1/\nu_B$, which gives rise to a periodic interference pattern. This multiwave interferometry phenomenon is similar to that described in [18], where Bloch oscillations are interpreted as periodic rephasing of the many WS components of a pure quasimomentum. In our multiwave interferometer, Raman transitions are used as a state labeling tool changing both the internal and external state of the atoms, allowing for an efficient detection based on the internal state populations [39–41], and not on the external state (position or momentum) [23,27,28,31]. This method gives interference fringes without any modulation of the lattice depth. Furthermore, atoms are in the same internal state during the whole interference evolution process; this makes the interferometric phase insensitive to light shifts induced by the trapping and Raman lasers, which means that this kind of multiwave interferometer could improve the potential measurement accuracy of the Bloch frequency.

II. THEORETICAL SIMULATION

In our system, we consider ^{87}Rb atoms trapped in a vertical one-dimensional (1D) optical lattice far detuned from the atomic resonance. The laser-cooled atoms loaded into the lattice experience a periodic potential $\hat{H}_l = U_0[1 - \cos(2k_l\hat{z})]/2$, which is superimposed to the gravitational potential $\hat{H}_g = -m_a g \hat{z}$. U_0 and k_l represent the lattice depth and wave number, respectively. The external eigenstates of the Hamiltonian $\hat{H}_{\text{total}} = \hat{H}_l + \hat{H}_g$ are given by the WS ladder of states $|W_m\rangle$ well known from the solid state physics [42]. The quantum number m is the well index which labels the different lattice sites in the vertical direction. As shown in Fig. 1(b), the energy difference corresponding to the increment of potential energy between two neighboring wells is $h\nu_B$. Considering the two internal hyperfine states $|g\rangle = |5^2S_{1/2}, F = 1, m_F = 0\rangle$ and $|e\rangle = |5^2S_{1/2}, F = 2, m_F = 0\rangle$, the two WS-ladder-like configurations corresponding to states $|g, W_m\rangle$ and $|e, W_m\rangle$ are shown in Fig. 1(b).

The spread of the atomic wave function $|W_m\rangle$ depends on the lattice depth [43]. In the case of a shallow depth ($U_0 < 5E_r$, where E_r is the recoil energy defined by $E_r/\hbar = \hbar k_l^2/2m_a = 2\pi \times 8$ kHz), the wave function can extend across a significant number of wells [43,44]. This delocalization allows resonant Raman transition induced tunneling between different lattice

*franck.pereira@obspm.fr

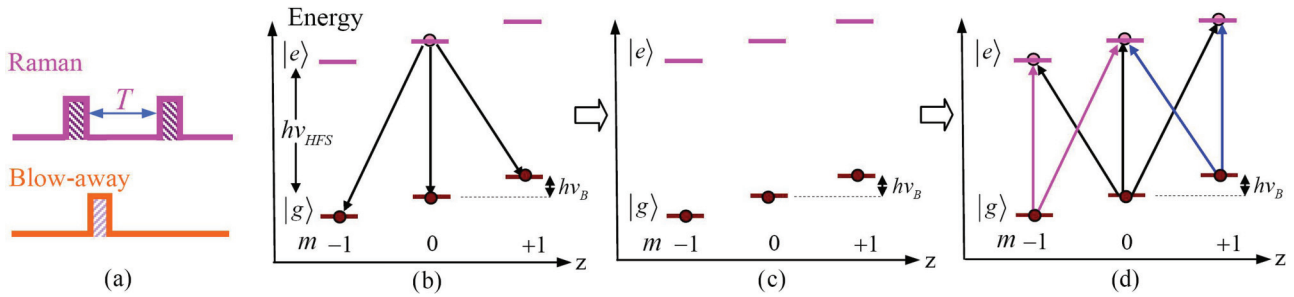

FIG. 1. (Color online) (a) Experimental sequence of the multiwave atom interferometer. (b)–(d) Evolution of two-level atoms with Wannier-Stark ladder states in a multiwave interferometer, where (b) represents the interaction with the first Raman pulse, (c) the free evolution after the blow-away pulse, and (d) the interaction with the last Raman pulse. ν_B is the Bloch frequency, ν_{HFS} is the hyperfine transition frequency between $|g\rangle = |5^2S_{1/2}, F = 1, m_F = 0\rangle$, and $|e\rangle = |5^2S_{1/2}, F = 2, m_F = 0\rangle$.

wells [36]. These transitions can be coherently driven by two-photon stimulated Raman transitions using counterpropagating vertical Raman beams, which can induce Rabi oscillations between $|g, W_m\rangle$ and $|e, W_{m'}\rangle$ either in the same well ($m = m'$) or in neighboring wells ($m \neq m'$). The Rabi frequency [36] is given by $\Omega_{\Delta m} = \Omega_{U_0=0}\langle W_m|e^{-ik_{eff}\hat{z}}|W_{m+\Delta m}\rangle$, where $\Omega_{U_0=0}$ is the two-photon Rabi frequency in free fall, and $k_{\mathrm{eff}} = k_{R1} + k_{R2} \approx 4\pi/\lambda_{\mathrm{Raman}}$ is the effective wave number with $\lambda_{\mathrm{Raman}} \approx 780$ nm. The Raman transitions change both the internal and external states, which can be observed by using a state selective detection technique.

We apply short Raman pulses with full laser power. In this case, the width (a few kHz) of the Raman pulse in the frequency domain is larger than ν_B ($\sim$568 Hz), which enables the spectrum to cover WS-state transitions between several adjacent sites. Atoms are initially in $|e, W_m\rangle$. A first Raman pulse of duration τ transfers the atoms to different adjacent lattice sites with different Δm [Fig. 1(b)]. A blow-away pulse is then used to clear the residual atoms in $|e, W_m\rangle$ states [Fig. 1(c)]. Each state $|g, W_{m'}\rangle$ evolves with its own frequency separated from the others by multiples of ν_B. The atomic state during the free evolution is

$$|\psi(t)\rangle = \left(\sum_{m=-M}^{M} {A_m}^2\right)^{-1/2} e^{i(\phi_R^1 + 2\pi\nu_{\mathrm{HFS}}t)} \times \sum_{m=-M}^{M} A_m e^{im\omega_B t}|g, m\rangle, \quad (1)$$

where $\phi_R^1 = \phi_{R1} - \phi_{R2}$ is the phase imprinted by the first Raman pulse, and A_m is the transition probability amplitude for each Δm transition. When atoms are superimposed in different WS states, the wave function $|\psi(t)\rangle$ evolves as a multimode matter wave [18]. After an evolution time T, a second Raman pulse identical to the first one is used to recombine the atoms [Fig. 1(d)]. In the limit of small excitation $\Omega_{\Delta m}\tau \ll \pi$, A_m is approximately proportional to $\Omega_{\Delta m}$, and the final state is

$$|\psi\rangle = Ce^{i(\phi_R^1 + 2\pi\nu_{\mathrm{HFS}}T)} \sum_{m=-M}^{M} A_m e^{im\omega_B T} \times \left(\sum_{m'=-M}^{M} e^{i\phi_R^2} A_{m'}|e, m + m'\rangle + B_m|g, m\rangle\right), \quad (2)$$

where C is a constant, ϕ_R^2 is the phase of the second Raman pulse, and B_m represents the probability amplitude of the remaining atoms staying in $|g, m\rangle$ due to the imperfect Raman transitions. The modulus square of the probability amplitude $|c_e|^2 = \sum_{m''=-2M}^{2M} |\langle e, W_{m''}|\psi\rangle|^2$ (where the new index indicator m'' covers every possible site after the two Raman pulses) can be written as

$$|c_e|^2 = C^2\left(\sum_{m=0}^{2M}\left|\sum_{m'=0}^{2M-|m|} A_{M-m'}A_{m+m'-M}e^{im'\omega_B T}\right|^2 + \sum_{m=-2M}^{-1}\left|\sum_{m'=0}^{2M-|m|} A_{m'-M}A_{M+m-m'}e^{-im'\omega_B T}\right|^2\right). \quad (3)$$

We notice that $|c_e|^2$ shows interferences with a period of $2\pi/\omega_B = 2h/(m_a g\lambda_l)$. This kind of periodic interference pattern is similar to the classical optical Fabry-Pérot interferometer. From previous work of that experiment [38–40], the coupling A_m is transition dependent, as the Rabi frequency depends on m. The theoretical interferometry pattern $|c_e|^2/|A_0|^4$ is shown in Fig. 2, where the number of lattice sites M is set to 2 and the coupling is $|A_{\pm2}|^2 : |A_{\pm1}|^2 : |A_0|^2 = 1 : 2 : 3$. Two neighboring peaks in Fig. 2 are separated by the Bloch period

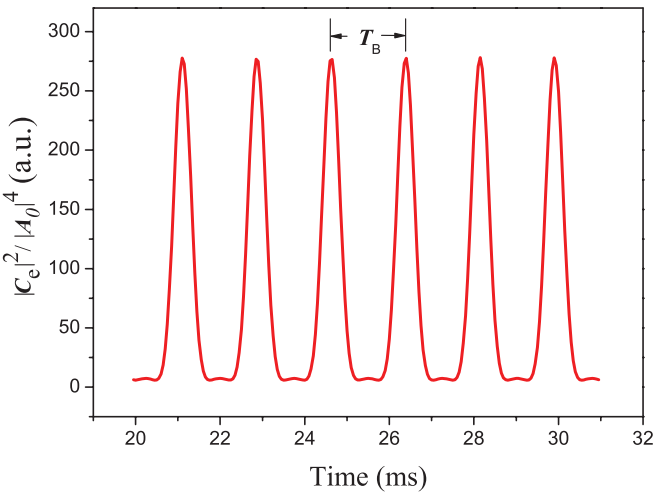

FIG. 2. (Color online) The theoretical atomic multiwave interference patterns with $M = 2$ and $|A_{\pm2}|^2 : |A_{\pm1}|^2 : |A_0|^2 = 1 : 2 : 3$.

$T_B = 2\pi/\omega_B$, which shows that such an atomic multiwave interferometer provides a method for measuring the Bloch frequency in a lattice.

III. EXPERIMENTS AND RESULTS

The experimental setup has already been described in [39,40]. A vertically retroreflected single mode and frequency doubled Nd: YVO4 laser ($\lambda_l = 532$ nm, $P = 8$ W, and beam waist ~ 700 μm on the atoms) is used to create the 1D optical lattice holding the atoms in the vertical direction. In order to confine the atoms in the horizontal direction, a well focused red detuned Yb fiber laser ($\lambda_I = 1064$ nm, $P \simeq 2$ W, beam waist ~ 180 μm localized on the atoms) is superimposed to the lattice providing a transverse dipole trap. Atoms are loaded into the mixed trap from a far red detuned molasses, and $\sim 10^5$ atoms with a temperature of 2 μK are distributed in thousands of adjacent sites in the fundamental Wannier-Stark band. The Raman transitions are driven by two counterpropagating beams at 780 nm circularly polarized, red detuned of 3 GHz from the D_2 resonant transition, and well aligned along the vertical direction. The Raman beams are collimated with an e^{-2} diameter of 5 mm and a total power ($P_{R1} + P_{R2}$) of 6 mW, which can drive a transition corresponding to $\Delta m = +8\nu_B$ with a Rabi frequency of 500 Hz at a well depth of $1.6E_r$. At the end of the 3D-MOT, the atoms in all the Zeeman sublevels of the $|5^2S_{1/2}, F = 2\rangle$ state are depumped to $|5^2S_{1/2}, F = 1\rangle$ and then optically pumped to state $|5^2S_{1/2}, F = 1, m_F = 0\rangle$ with 95% efficiency. We then use a microwave π pulse to transfer the atoms to the aimed state of $|5^2S_{1/2}, F = 2, m_F = 0\rangle$. After the state preparation, the atoms are ready to interact with the Raman pulses to realize the multiwave interferometer. Finally, a time-of-flight fluorescence state selective detection is applied to determine the populations in the two hyperfine states after the release of the atoms from the trap.

To demonstrate the multiwave atom interferometer in the lattice, a first Raman pulse with a duration of 200 μs is used to transfer the atoms to state $|5^2S_{1/2}, F = 1, m_F = 0\rangle$ into a superposition of multiple adjacent lattice sites. The coupling strength corresponding to transitions to different lattice sites depends on the lattice depths U_0 and on the Raman frequency $\nu_{\mathrm{HFS}} + \delta$, where the detuning δ can be tuned at zero or at a multiple of ν_B. After optimizations of the experimental parameters, the Raman frequency and the lattice depth are chosen as $\nu_{\mathrm{HFS}} + 8\nu_B$ and $1.6E_r$, respectively, and the fraction of Raman excitation is limited to 20%. After the first Raman pulse, a blow-away pulse is used to clear the remaining atoms in the upper hyperfine state $|5^2S_{1/2}, F = 2\rangle$. The second Raman pulse identical to the first one is employed after a time delay T to recombine the atoms. By scanning T, a multiwave atomic interferometry pattern with a contrast of 19% is obtained as shown in Fig. 3(a), which exhibits the expected period $T_B = 1/\nu_B$. We studied the evolution of the fringe contrast when increasing the integration time T as shown in Fig. 3(b). We observe a rather linear decay of the contrast with T due to some decoherence in the evolution process. For example, when we set $T = 850$ ms, we observe coherent evolution for more than 500 Bloch periods, but the contrast decreases to 6%.

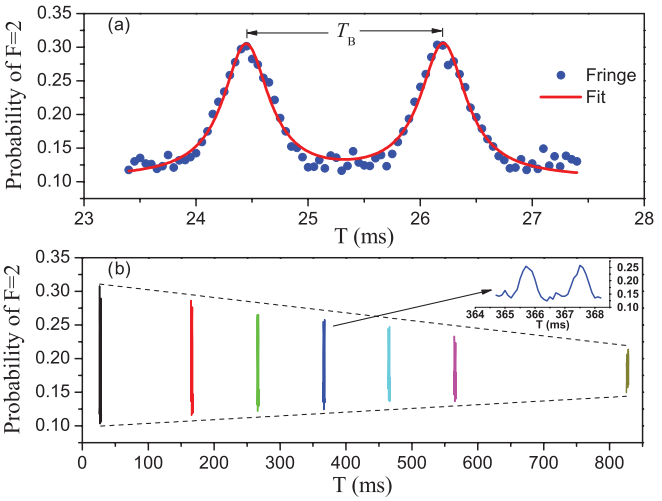

FIG. 3. (Color online) (a) A typical multiwave atomic interferometry pattern obtained in the lattice with ten times average. (b) The contrast decreases when increasing the integration time T.

The periodic feature of the multiwave atomic interferometry pattern provides a method for measuring the Bloch frequency. A straightforward way to get the Bloch frequency is to fit the pattern directly to find the separation between the neighboring peaks. A least-square fitting of the fringe with Lorentzian function gives a value of $T_B = 1.759(1)$ ms [Fig. 3(a)], corresponding to a Bloch frequency of $\nu_B = 568.5(3)$ Hz, which is consistent with [41]. We can also get the Bloch frequency by calculating the fast Fourier transform (FFT) of the fringes with long time data accumulation. We record the fringe data by scanning T from 22 to 200 ms with a step of 0.1 ms. The FFT of this scan is shown in Fig. 4. The second harmonic frequency component given by the FFT data is found to be 1136.74(5) Hz, corresponding to $\nu_B = 568.37(3)$ Hz, which is consistent with the result of the least-square fitting method and [41]. The uncertainties of ν_B given here are the statistical error.

The relative resolution of Bloch frequency for the atomic multiwave interferometer is given by $\delta\nu_B/\nu_B = \delta T/T =$

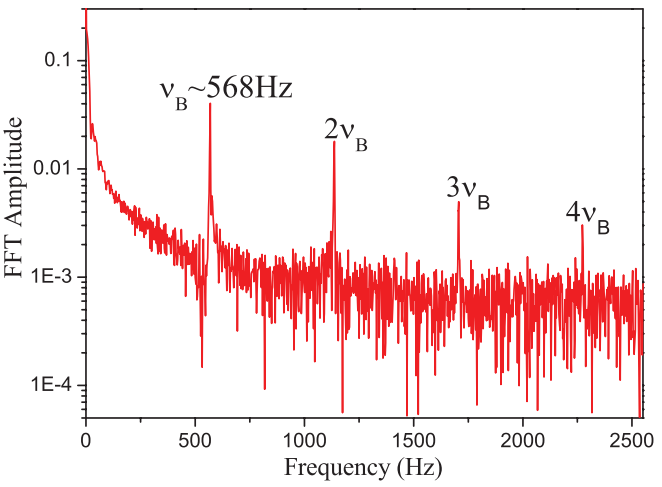

FIG. 4. (Color online) The FFT of fringes obtained from the pattern data by scanning T from 22 to 200 ms.

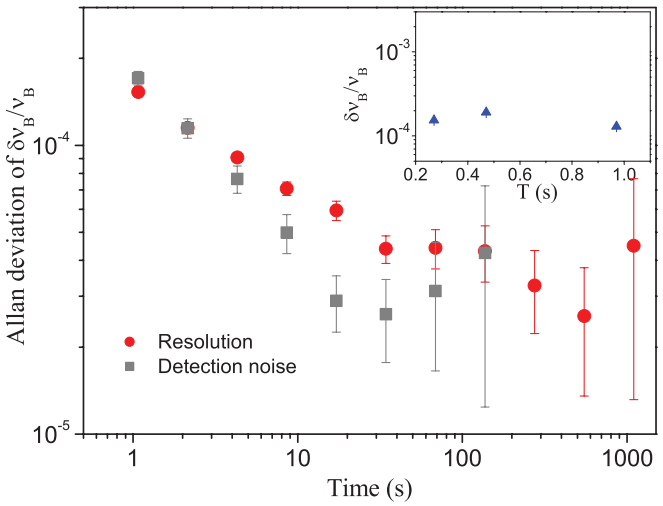

FIG. 5. (Color online) The Allan standard deviation of the Bloch frequency measurements by the atomic multiwave interferometer. The inset is the short term (at 1 s) sensitivity vs the integration time T. These data are obtained for $T = 0.27$ s, $T_t = 0.3$ s, $T = 0.47$ s, $T_t = 0.5$ s, and $T = 0.9$ s, $T_t = 1$ s, where T_t is the total trapping time.

$\delta P_e/(kN_BT_B)$, where $k = dP_e/dT$ is the slope near the middle of the fringe sides, δP_e is the transition probability noise, and N_B is the number of fringes. In order to get the optimized sensitivity, the probability P_e is recorded continuously at mid-fringe, and the resolution of the Bloch frequency measurement can be given by $\delta\nu_B/\nu_B = \delta P_e/(kT)$. An efficient way to increase the sensitivity is to use a larger evolution time T. However, when increasing T, the contrast decreases due to decoherence [Fig. 3(b)], leading to a decrease of signal-to-noise ratio. Moreover, an increase of T necessitates a longer trapping time T_t, leading to a loss of atoms [41] and to the increase of the fluctuations of P_e as the experiment is detection noise limited. The short-term sensitivity (at 1 s) for different T is shown in the inset of Fig. 5, where the sensitivity remains quite constant for T larger than 270 ms. This points out the balance between the three main parameters in these measurements: When the trapping time gets longer, N_B is increased, while k decreases and δP_e increases. The optimized parameter $T = 270$ ms is selected.

From consecutive measurements of the transition probability at mid-fringe, we estimate the short-term sensitivity on the measurement of Bloch frequency, as illustrated by the red points in Fig. 5. The $\delta\nu_B/\nu_B$ can reach a resolution of 1.5×10^{-4} at 1 s, and it decreases to 2.6×10^{-5} after 550 s of integration time. This gives a sensitivity on the gravitational acceleration measurement at a level of 10^{-5}. We plotted as well the equivalent resolution deduced from the detection noise (gray squares in Fig. 5), showing that the measurements are detection noise limited: Only about 4×10^4 atoms are left after the first Raman pulse and the blow-away beam due to the low coupling efficiency of the transitions. The signal-to-noise ratio is thus greatly reduced by this loss of atoms, which limits the resolution of the interferometer [41]. Due to this limitation, the short-term sensitivity of the multiwave interferometer at 1 s is about one order less than the Ramsey-Raman and Accordion interferometer previously demonstrated in [41].

IV. CONCLUSION

In conclusion, we have experimentally demonstrated an atomic multiwave interferometer with stimulated Raman transitions and trapped atoms, which provides a method for the measurement of Bloch frequency in a shallow optical lattice. The resolution on ν_B measurement is presently detection noise limited due to the low atom number ($N \sim 4 \times 10^4$), and this resolution could be improved by increasing the atom number in the mixed trap. As atoms are in the same internal state, this kind of multiwave interferometer is theoretically insensitive to light shifts, and it could be a potential scientific tool for precision measurements, such as for short-range forces measurement or as a gravimeter.

ACKNOWLEDGMENTS

This research is carried out within the project iSense, which acknowledges the financial support of the Future and Emerging Technologies (FET) programme within the Seventh Framework Program for Research of the European Commission, under FET-Open Grant No. 250072. We also gratefully acknowledge support from Ville de Paris [Emergence(s) program] and IFRAF. M.K.Z. thanks the FFCSA, CSC, and CNSF (Grant No. 11205064) for financial support.

[1] A. D. Cronin, J. Schmiedmayer, and D. E. Pritchard, Rev. Mod. Phys. **81**, 1051 (2009).
[2] K. Bongs and K. Sengstock, Rep. Prog. Phys. **67**, 907 (2004).
[3] M. Kasevich and S. Chu, Phys. Rev. Lett. **67**, 181 (1991).
[4] C. J. Bordé, Phys. Lett. A **140**, 10 (1989).
[5] A. Peters, K. Y. Chung, and S. Chu, Nature (London) **400**, 849 (1999).
[6] P. Cheinet, F. Pereira dos Santos, T. Petelski, J. Le Gouët, J. Kim, K. Therkildsen, A. Clairon, and A. Landragin, Appl. Phys. B **84**, 643 (2006).
[7] J. Le Gouët, T. Mehlstäubler, J. Kim, S. Merlet, A. Clairon, A. Landragin, and F. Pereira dos Santos, Appl. Phys. B **92**, 133 (2008).
[8] Q. Bodart, S. Merlet, N. Malossi, F. Pereira dos Santos, P. Bouyer, and A. Landragin, Appl. Phys. Lett. **96**, 134101 (2010).
[9] M. K. Zhou, Z. K. Hu, X. C. Duan, B. L. Sun, L. L. Chen, Q. Z. Zhang, and J. Luo, Phys. Rev. A **86**, 043630 (2012).
[10] R. Charrière, M. Cadoret, N. Zahzam, Y. Bidel, and A. Bresson, Phys. Rev. A **85**, 013639 (2012).
[11] F. Impens and C. J. Bordé, Phys. Rev. A **80**, 031602 (2009).
[12] M. Weitz, T. Heupel, and T. W. Hänsch, Phys. Rev. Lett. **77**, 2356 (1996).
[13] S. Fray, C. A. Diez, T. W. Hänsch, and M. Weitz, Phys. Rev. Lett. **93**, 240404 (2004).

[14] B. Barrett, I. Chan, and A. Kumarakrishnan, Phys. Rev. A **84**, 063623 (2011).
[15] H. Hinderthür, F. Ruschewitz, H. J. Lohe, S. Lechte, K. Sengstock, and W. Ertmer, Phys. Rev. A **59**, 2216 (1999).
[16] M. Robert de Saint Vincent, J. P. Brantut, C. J. Bordé, A. Aspect, T. Bourdel, and P. Bouyer, Europhys. Lett. **89**, 10002 (2010).
[17] K. J. Hughes, J. H. T. Burke, and C. A. Sackett, Phys. Rev. Lett. **102**, 150403 (2009).
[18] Q. Thommen, J. C. Garreau, and V. Zehnlé, Phys. Rev. A **65**, 053406 (2002).
[19] M. Gustavsson, E. Haller, M. J. Mark, J. G. Danzl, R. Hart, A. J. Daley, and H. C. Nägerl, New J. Phys. **12**, 065029 (2010).
[20] M. G. Tarallo, N. Poli, F. Wang, and G. M. Tino, Eur. Phys. J. Spec. Top. **217**, 207 (2013).
[21] M. Takamoto, F. L. Hong, R. Higashi, and H. Katori, Nature (London) **435**, 321 (2005).
[22] A. Derevianko and H. Katori, Rev. Mod. Phys. **83**, 331 (2011).
[23] P. Cladé, E. de Mirandes, M. Cadoret, S. Guellati-Khélifa, C. Schwob, F. Nez, L. Julien, and F. Biraben, Phys. Rev. Lett. **96**, 033001 (2006).
[24] G. Ferrari, N. Poli, F. Sorrentino, and G. M. Tino, Phys. Rev. Lett. **97**, 060402 (2006).
[25] J. J. Garcia-Ripoll, M. A. Martin-Delgado, and J. I. Cirac, Phys. Rev. Lett. **93**, 250405 (2004).
[26] E. Peik, M. Ben Dahan, I. Bouchoule, Y. Castin, and C. Salomon, Phys. Rev. A **55**, 2989 (1997).
[27] K. Madison, C. Bharucha, P. Morrow, S. Wilkinson, Q. Niu, B. Sundaram, and M. Raizen, Appl. Phys. B **65**, 693 (1997).
[28] M. Gustavsson, E. Haller, M. J. Mark, J. G. Danzl, G. Rojas-Kopeinig, and H.-C. Nägerl, Phys. Rev. Lett. **100**, 080404 (2008).
[29] H. J. Briegel, T. Calarco, D. Jaksch, J. I. Cirac, and P. Zoller, J. Mod. Opt. **47**, 415 (2000).
[30] P. Cladé, S. Guellati-Khélifa, C. Schwob, F. Nez, L. Julien, and F. Biraben, Europhys. Lett. **71**, 730 (2007).
[31] N. Poli, F.-Y. Wang, M. G. Tarallo, A. Alberti, M. Prevedelli, and G. M. Tino, Phys. Rev. Lett. **106**, 038501 (2011).
[32] M. Cadoret, E. de Mirandes, P. Cladé, S. Guellati-Khélifa, C. Schwob, F. Nez, L. Julien, and F. Biraben, Phys. Rev. Lett. **101**, 230801 (2008).
[33] R. Bouchendira, P. Cladé, S. Guellati-Khélifa, F. Nez, and F. Biraben, Phys. Rev. Lett. **106**, 080801 (2011).
[34] I. Carusotto, L. Pitaevskii, S. Stringari, G. Modugno, and M. Inguscio, Phys. Rev. Lett. **95**, 093202 (2005).
[35] S. Dimopoulos and A. A. Geraci, Phys. Rev. D **68**, 124021 (2003).
[36] P. Wolf, P. Lemonde, A. Lambrecht, S. Bize, A. Landragin, and A. Clairon, Phys. Rev. A **75**, 063608 (2007).
[37] A. Derevianko, B. Obreshkov, and V. A. Dzuba, Phys. Rev. Lett. **103**, 133201 (2009).
[38] S. Pélisson, R. Messina, M. C. Angonin, and P. Wolf, Phys. Rev. A **86**, 013614 (2012).
[39] Q. Beaufils, G. Tackmann, X. Wang, B. Pelle, S. Pelisson, P. Wolf, and F. P. dos Santos, Phys. Rev. Lett. **106**, 213002 (2011).
[40] G. Tackmann, B. Pelle, A. Hilico, Q. Beaufils, and F. Pereira dos Santos, Phys. Rev. A **84**, 063422 (2011).
[41] B. Pelle, A. Hilico, G. Tackmann, Q. Beaufils, and F. Pereira dos Santos, Phys. Rev. A **87**, 023601 (2013).
[42] G. Nenciu, Rev. Mod. Phys. **63**, 91 (1991).
[43] R. Messina, S. Pélisson, M. C. Angonin, and P. Wolf, Phys. Rev. A **83**, 052111 (2011).
[44] F. Bloch, Z. Phys **52**, 555 (1929).